Metabolic Engineering 30 (2015) 130–140

Contents lists available at ScienceDirect

Metabolic Engineering

journal homepage: www.elsevier.com/locate/ymben

Functional expression of a heterologous nickel-dependent, ATP-independent urease in *Saccharomyces cerevisiae*

N. Milne, M.A.H. Luttik, H.F. Cueto Rojas, A. Wahl, A.J.A. van Maris, J.T. Pronk, J.M. Daran *

Department of Biotechnology, Delft University of Technology, Julianalaan 67, 2628 BC Delft, The Netherlands

ARTICLE INFO

Article history:
Received 26 February 2015
Received in revised form
18 May 2015
Accepted 21 May 2015
Available online 30 May 2015

Keywords:
Saccharomyces cerevisiae
ATP-independent urease
Ni-dependent enzyme
ATP conservation
Nitrogen metabolism
Physiology

ABSTRACT

In microbial processes for production of proteins, biomass and nitrogen-containing commodity chemicals, ATP requirements for nitrogen assimilation affect product yields on the energy producing substrate. In *Saccharomyces cerevisiae*, a current host for heterologous protein production and potential platform for production of nitrogen-containing chemicals, uptake and assimilation of ammonium requires 1 ATP per incorporated NH_3. Urea assimilation by this yeast is more energy efficient but still requires 0.5 ATP per NH_3 produced. To decrease ATP costs for nitrogen assimilation, the *S. cerevisiae* gene encoding ATP-dependent urease (*DUR1,2*) was replaced by a *Schizosaccharomyces pombe* gene encoding ATP-independent urease (*ure2*), along with its accessory genes *ureD*, *ureF* and *ureG*. Since *S. pombe ure2* is a Ni^{2+}-dependent enzyme and *Saccharomyces cerevisiae* does not express native Ni^{2+}-dependent enzymes, the *S. pombe* high-affinity nickel-transporter gene (*nic1*) was also expressed. Expression of the *S. pombe* genes into *dur1,2*Δ *S. cerevisiae* yielded an in vitro ATP-independent urease activity of 0.44 ± 0.01 μmol min^{-1} mg $protein^{-1}$ and restored growth on urea as sole nitrogen source. Functional expression of the Nic1 transporter was essential for growth on urea at low Ni^{2+} concentrations. The maximum specific growth rates of the engineered strain on urea and ammonium were lower than those of a *DUR1,2* reference strain. In glucose-limited chemostat cultures with urea as nitrogen source, the engineered strain exhibited an increased release of ammonia and reduced nitrogen content of the biomass. Our results indicate a new strategy for improving yeast-based production of nitrogen-containing chemicals and demonstrate that Ni^{2+}-dependent enzymes can be functionally expressed in *S. cerevisiae*.

1. Introduction

Industrial biotechnology can contribute to the transition to sustainable production of fuels and chemicals from renewable agricultural feedstock's by enabling efficient microbial conversion of carbohydrates into a wide range of economically relevant compounds (Hong and Nielsen, 2012). To be competitive with petrochemical processes, it is essential that microbial conversions are optimized to achieve maximum yields and productivities.

Microbial production of large-volume nitrogen-containing chemicals such as amino acids (Wu, 2009) and diamines (Lucet et al., 1998) is currently based on bacteria, and in particular on *Corynebacterium glutamicum* and *Escherichia coli* (Hermann, 2003; Ikeda, 2003; Qian et al., 2009; Qian et al., 2011). Efficient export systems for nitrogen-containing products and high product titres contribute to the popularity of these bacterial hosts (Hermann, 2003; Ikeda, 2003). Current microbial biotechnology processes for production on nitrogenous organic compounds are, without exception, aerobic (Hermann, 2003). Aeration of large industrial bioreactors is expensive and respiratory conversion of growth substrates causes reduced product yields. Moreover, aerobic respiration is strongly exergonic which, in large reactors, leads to extra cooling costs. Large-scale microbial production processes should therefore, whenever permitted by thermodynamics and biochemistry of the metabolic pathways involved, be performed under anaerobic conditions. To achieve a high product yield on substrate, the ATP yield from the product pathway should ideally be low, but sufficient to achieve a situation in which high catabolic fluxes are needed to meet ATP requirements for maintenance and growth (de Kok et al., 2012; Weusthuis et al., 2011). Such a situation is exemplified by anaerobic alcoholic fermentation of glucose by *S. cerevisiae*, which yields only 2 mol ATP per mol of glucose. In contrast, completely respiratory dissimilation of glucose by *S. cerevisiae*, which has a P/O ratio of 1.0 (Bakker et al., 2001), yields ca. 16 mol ATP per mol of glucose and, consequently, results in much higher biomass yields. Engineered *S. cerevisiae* strains are intensively studied and applied for production of

* Corresponding author.
E-mail address: j.g.daran@tudelft.nl (J.M. Daran).

http://dx.doi.org/10.1016/j.ymben.2015.05.003

organic compounds (Hong and Nielsen, 2012), but its use for production of nitrogen-containing compounds is so far restricted to high-value compounds such as proteins and peptides, most notably human insulin (Cousens et al., 1987; Ostergaard et al., 2000; Walsh, 2005).

Especially in the design of anaerobic processes for production of low-molecular weight nitrogen-containing compounds (e.g. amino acids) by *S. cerevisiae*, indicated ATP costs for uptake and assimilation of nitrogen sources should be minimized. Ammonium and urea are two cheap nitrogen sources commonly used in large-scale fermentation processes (Albright, 2000; Xun Yao, 2014). In *S. cerevisiae*, ATP is expended in the initial steps of the assimilation of both these compounds. Import of NH_4^+ via the Mep1, Mep2 and Mep3 uniporters (Marini et al., 1997) is followed by its intracellular dissociation into NH_3, which is used for biomass/product formation, and a proton, which must be exported in order to maintain homoeostasis of the proton motive force (de Kok et al., 2012). In *S. cerevisiae*, this process is catalysed by the ATP-dependent plasma-membrane H^+-ATPase Pma1 with a stoichiometry of 1 ATP per proton (de Kok et al., 2012). The energy dependency of ammonium uptake in *S. cerevisiae* makes it extremely challenging to improve ATP utilization. Per mole of nitrogen, urea (NH_2–CO–NH_2) is often cheaper than ammonium and, in contrast to ammonium, its assimilation does not cause medium acidification (Hensing et al., 1995). In urea-sufficient cultures of *S. cerevisiae*, urea uptake is not proton-coupled (Cooper and Sumrada, 1975) but ATP is expended during its conversion to ammonia by urea amidolyase (urease) encoded by *DUR1,2* (Fig. 1). This urease converts urea into two molecules of ammonia and one mole of CO_2 in a two-step reaction that involves ATP hydrolysis (Mobley et al., 1995), resulting in a cost of 0.5 ATP per mol NH_3 assimilated into product. In many other micro-organisms, urea can be converted into two molecules of ammonia in a single, ATP-independent reaction (Genbauffe and Cooper, 1986) (Fig. 1).

Although clearly beneficial for the ATP economy of the cell during growth on urea, the use of ATP-independent urease introduces the complication that all known ATP-independent urease enzymes require nickel insertion at the active site for catalytic activity. A notable exception is the *Helicobacter mustelae* urease, which requires iron instead of nickel, presumably to allow this pathogen to inhabit the low-nickel environment of its host *Mustela putorius furo* (Carter et al., 2011). In the fission yeast *Schizosaccharomyces pombe*, ATP-independent urea assimilation is catalysed by the nickel-requiring enzyme Ure2, whose activity requires the three accessory proteins UreD, UreF and UreG. UreD and UreF have been proposed to function as chaperones to incorporate nickel into the Ure2 enzyme active site and to assist in protein folding, while UreG is thought to deliver nickel from the cell membrane to the urease enzyme (Bacanamwo et al., 2002). The high-affinity nickel transporter Nic1 is involved in Ni^{2+} uptake across the *S. pombe* plasma membrane (Eitinger et al., 2000). The roles of the proteins involved in ATP-independent urea assimilation have been predominantly elucidated in *Klebsiella aerogenes* and are homologous across distantly related species (Mobley et al., 1995).

The aim of the present study was to investigate whether the native ATP-dependent urease of *S. cerevisiae* can be functionally replaced by a heterologous ATP-independent and nickel-requiring urease. To this end we sought to replace the native ATP-dependent urea assimilation gene *DUR1,2* with the complete ATP-independent urea assimilation system from *S. pombe* (Bacanamwo et al., 2002; Eitinger et al., 2000; Mobley et al., 1995; Navarathna et al., 2010). The functionality of the heterologous urease was characterized in vivo and in vitro. To investigate the impact of these genetic modifications on yeast physiology, growth of engineered strains and a *DUR1,2* reference strain was compared during growth on urea and ammonium-containing media and at different nickel concentrations in batch and chemostat cultures.

2. Materials and methods

2.1. Media, strains and maintenance

All *S. cerevisiae* strains used in this study (Table 1) were derived from the CEN.PK strain family background (Entian and Kötter, 2007; Nijkamp et al., 2012). The *S. pombe* CBS7264 strain was obtained from CBS-KNAW (Utrecht, The Netherlands [http://www.cbs.knaw.nl/]). Frozen stocks of *E. coli* and *S. cerevisiae* were prepared by addition of glycerol (30% (v/v)) to exponentially growing cells and aseptically storing 1 mL aliquots at −80 °C. Cultures were grown in synthetic medium according to the following recipes. Ammonium sulphate synthetic medium (SMA) was prepared with 3 g/L KH_2PO_4, 0.5 g/L $MgSO_4 7H_2O$ and 5 g/L $(NH_4)_2SO_4$ (Verduyn et al., 1992). Urea synthetic medium (SMU) was prepared with 6.6 g/L K_2SO_4, 3 g/L KH_2PO_4, 0.5 g/L $MgSO_4$, $7H_2O$ and 2.3 g/L $CO(NH_2)_2$. Serine synthetic medium (SMS) was prepared with 6.6 g/L K_2SO_4, 3 g/L KH_2PO_4, 0.5 g/L $MgSO_4$, $7H_2O$ and 5 g/L serine. Histidine synthetic medium was prepared with 6.6 g/L K_2SO_4, 3 g/L KH_2PO_4, 0.5 g/L $MgSO_4$, $7H_2O$ and 10 mg/L histidine. In all cases unless stated otherwise 20 g/L glucose and appropriate growth factors were added according to (Pronk, 2002), and the pH adjusted to 5.0. If required for anaerobic growth Tween-80 (420 mg/L) and ergosterol (10 mg/L) were added. Synthetic medium agar plates were prepared as described above but with the addition of 20 g/L agar (Becton Dickinson B.V. Breda, The Netherlands)

2.2. Strain construction

S. cerevisiae strains were transformed using the lithium acetate method according to (Gietz and Woods, 2002). The *DUR1,2* deletion cassette was constructed by amplifying the KanMX4 cassette from the vector pUG6 (Guldener et al., 1996) using primers with added homology to the upstream and downstream regions of *DUR1,2* (DUR1,2 KO Fwd/DUR1,2 KO Rev) (Table 3). PCR amplification was performed using Phusion® Hot Start II High Fidelity Polymerase (Thermo scientific, Waltham, MA) according to the manufactures instructions using HPLC or PAGE purified, custom synthesized oligonucleotide primers (Sigma Aldrich, Zwijndrecht, The Netherlands) in a Biometra TGradient Thermocycler (Biometra, Gottingen, Germany). The KanMX4 deletion cassette was transformed into CEN.PK113-5D (*ura3-52*) yielding strain IMK504 (*ura3-52, dur1,2*Δ) and transformants were selected on SMA agar with 200 mg/L G418 (Sigma Aldrich) and 150 mg/L uracil. Deletion of *DUR1,2* was confirmed by PCR on genomic DNA preparations using the diagnostic primers listed under "Primers for verification of knockout cassettes" in Table 3. Diagnostic PCR was performed using DreamTaq (Thermo scientific) and desalted primers (Sigma Aldrich) in a Biometra TGradient Thermocycler (Biometra). Genomic DNA was prepared using a YeaStar Genomic DNA kit (Zymo Research, Orange, CA).The prototrophic *dur1,2*Δ strain IME184 was constructed by transformation of IMK504 with plasmid p426GPD (2 μm, *URA3*) (Mumberg et al., 1995). Transformants were selected on SMA agar.

Construction of the ATP-independent urease strain IMY082 was achieved using in vivo vector assembly by homologous recombination according to (Kuijpers et al., 2013). DNA coding sequences of *S. pombe ure2* (NM_001020242), *ureD* (NM_001018767.2), *ureF* (NM_001020298.2), *ureG* (NM_001023020.2) and *nic1* (NM_001022671.2) were codon optimized for *S. cerevisiae* using the JCat algorithm (Grote et al., 2005). Custom synthesized cassettes cloned into the vector pUC57 (GenBank accession number: Y14837.1) were provided by BaseClear (Leiden, The Netherlands)

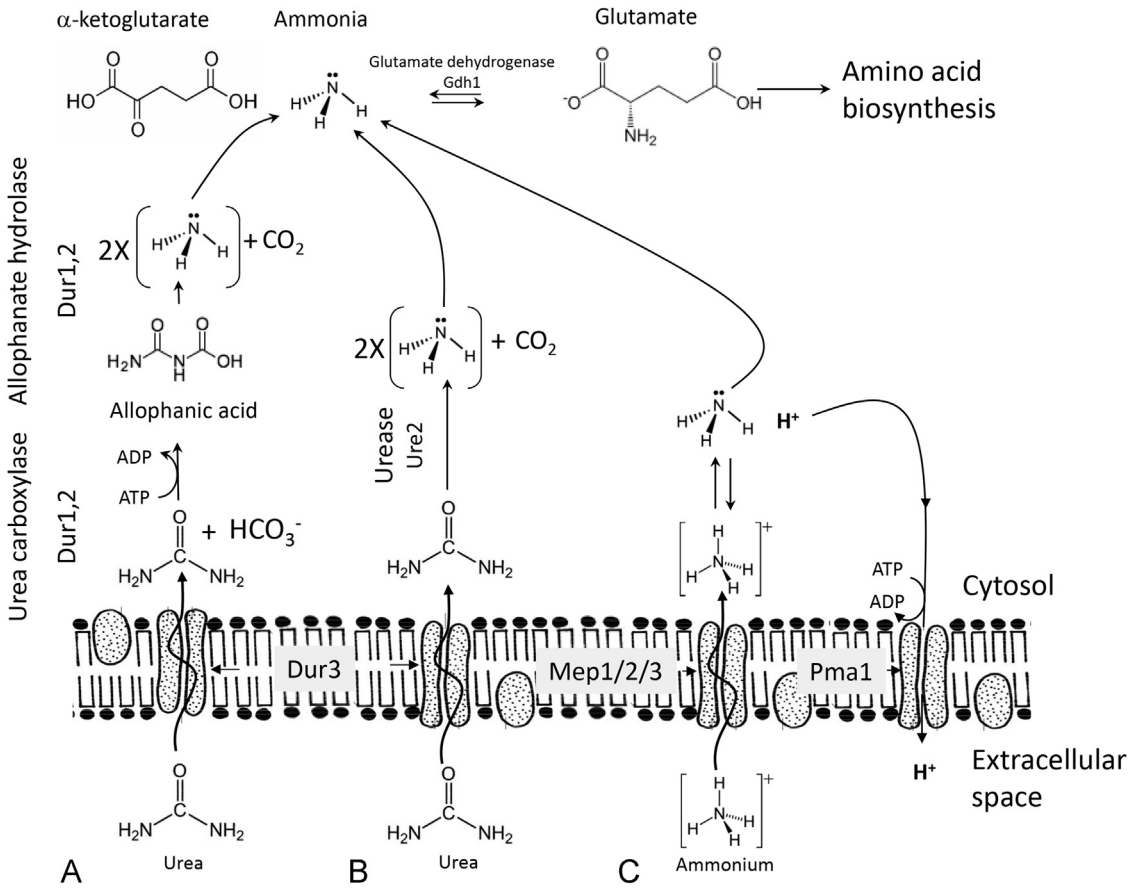

Fig. 1. Overview of native urea and ammonium assimilation in *S. cerevisiae* and proposed strategy for engineering ATP-independent urea assimilation into this yeast. (A) Native ATP-dependent urea assimilation involves urea crossing the cell membrane by either passive/facilitated diffusion or via the Dur3 urea active transporter. In the cytoplasm the urea carboxylase activity of the bi-functional enzyme Dur1,2 converts urea to allophanic acid at the expense of 1 ATP. The allophonic acid is then converted to 2 molecules of NH_3 by the allophanate hydrolase activity of Dur1,2. (B) Heterologous ATP-independent urea assimilation involves urea entering the cytoplasm as previously described then being converted to 2 molecules of NH_3 in an ATP-independent manner. In both cases CO_2 is produced as a by-product. **C**. Ammonium assimilation involves the import of the charged ammonium molecule (NH_4^+) into the cell by one of three ammonium permeases (Mep1/2/3). At the close to neutral pH in the cytoplasm, NH_4^+ dissociates forming NH_3 and the corresponding H^+. In order to maintain pH homoeostasis and proton motive force the proton generated is exported from the cell by the H^+-ATPase Pma1 at the expensive of 1 ATP. In all cases, the resulting NH_3 molecules can then be incorporated into amino acids, via reductive amination of α-ketoglutarate, yielding glutamate.

Table 1
Strains used in this study.

Name	Relevant genotype	Origin
Saccharomyces cerevisiae		
CEN.PK113-7D	MATa *URA3 HIS3 LEU2 TRP1 MAL2-8c SUC2*	Entian and Kötter (2007) and Nijkamp et al. (2012)
CEN.PK113-5D	MATa *ura3-52 HIS3 LEU2 TRP1 MAL2-8c SUC2*	Entian and Kötter (2007) and Nijkamp et al. (2012)
IME140	MATa *ura3-52 HIS3 LEU2 TRP1 MAL2-8c SUC2*+p426GPD (2 μm *URA3*)	Kozak et al., (2014b) and Nijkamp et al. (2012)
IMK504	MATa *ura3-52 HIS3 LEU2 TRP1 MAL2-8c SUC2 dur1,2Δ: loxP*-KanMX4-*loxP*	This study
IME184	MATa *ura3-52 HIS3 LEU2 TRP1 MAL2-8c SUC2 dur1,2Δ: loxP*-KanMX4-*loxP* + p426GPD (2μm *URA3*)	This study
IMY082	MATa *ura3-52 HIS3 LEU2 TRP1 MAL2-8c SUC2 dur1,2Δ: loxP*-KanMX4-*loxP* + pUDC121	This study
IMZ459	MATa *ura3-52 HIS3 LEU2 TRP1 MAL2-8c SUC2 dur1,2Δ: loxP*-KanMX4-*loxP* + pUDE266	This study
Schizosaccharomyces pombe		
S. pombe 7264	*Schizosaccharomyces pombe* wild-type strain	CBS-KNAW[a]

[a] Utrecht, The Netherlands [http://www.cbs.knaw.nl/].

containing the codon optimized genes, flanked by strong constitutive promoters and terminators from the *S. cerevisiae* glycolytic pathway. Each cassette was further flanked with 60 bp tags (labelled A through I) with homology to an adjacent cassette. These tags have no significant homology to the *S. cerevisiae* genome ensuring that each cassette can only recombine with an adjacent cassette using homologous recombination (Kuijpers et al., 2013). Custom synthesis resulted in plasmids pUD215 (B-$TDH3_p$-*ure2*-$CYC1_t$-C), pUD216 (G-$PGK1_p$-*nic1*-$TEF1_t$-I), pUD217 (D-$TEF1_p$-*ureD*-$PGK1_t$-E), pUD218 (E-$ADH1_p$-*ureF*-$PYK1_t$-F) and pUD219 (C-$TPI1_p$-*ureG*-$ADH1_t$-D) (Table 2). Each plasmid was transformed into chemically competent *E. coli* (T3001, Zymo Research) according to the manufacturer's instructions, and the gene sequences confirmed by Sanger sequencing (BaseClear). Also included were plasmids with cassettes encoding a *URA3* yeast selection marker (pUD192: A-*URA3*-B), a *CEN6-ARS4* yeast replicon (pUD193: F-*CEN6-ARS4*-G), and a fragment containing an AmpR ampicillin resistance marker and *E. coli* origin of replication (pUD195:

Table 2
Plasmids used in this study. CO: codon optimized.

Name	Characteristics	Origin
pUC57	Delivery vector used for blunt cloning of custom synthesized gene cassettes	BaseClear, Leiden, The Netherlands
pUD215	pUC57 + *TDH3$_p$-COure2-CYC1$_t$*	This study
pUD216	pUC57 + *PGK1$_p$-COnic1-TEF1$_t$*	This study
pUD217	pUC57 + *TEF1$_p$-COureD-PGK1$_t$*	This study
pUD218	pUC57 + ADH1$_p$-*COureF*-PYK1$_t$	This study
pUD219	pUC57 + TPI1$_p$-*COureG*-ADH1$_t$	This study
pUD192	pUC57 + *URA3*	Kozak et al. (2014b) and Kozak et al. (2014a)
pUD193	pUC57 + *CEN6-ARS4*	Kozak et al. (2014b)
pUD195	*AmpR, E. coli* replicon	Kozak et al. (2014a)
p426GPD	2 μm ori, *URA3, TDH3*$_p$-CYC1$_t$	Mumberg et al. (1995)
pUG6	PCR template for *loxP*-KanMX4-*loxP* cassette	Guldener et al. (1996)
pUDC121	*CEN6-ARS4* ori, *AmpR, URA3, TDH3$_p$-COure2-CYC1t, TPI1 $_p$ -COureG-ADH1$_t$, TEF1$_p$-COureD-PGK1$_{tt}$, ADH1$_p$-COureF-PYK1$_t$, PGK1$_p$-COnic1-TEF1$_t$*	This study
pUDE266	*CEN6-ARS4* ori, *AmpR, URA3, TDH3$_p$-COure2-CYC1t, TPI1$_p$-COureG-ADH1$_t$, TEF1$_p$-COureD-PGK1$_t$, ADH1$_p$-COureF-PYK1$_t$*	This study

Table 3
Oligonucleotide primers used in this study.

Name	Sequence (5′→3′)
Primers for knockout cassettes	
DUR1,2 KO Fwd	GTCACAATAAATTTCAGTTTTGATTAAAAAATGACAGTTAGTTCCGATACAACTGAGATCGAGGTTTAGCCATGTCAGCT-GAAGCTTCGTACGC
DUR1,2 KO Rev	GTCACAATAAATTTCAGTTTTGATTAAAAAATGACAGTTAGTTCCGATACAACTGAGATCGAGGTTTAGCCATGTCAGCT-GAAGCTTCGTACGC
Primers for verification of knockout cassettes	
DUR1,2 Upstream Fwd	CGCCACGCATCTTTGGCTGCATTTCG
DUR1,2 Downstream Rev	ATGCCTTGTAGTCGCCACCTGCTTCCTC
DUR1,2 Internal Fwd	GTCTGGCCGCATCTTCTGAGGTTCC
DUR1,2 Internal Rev	TCTACCAGAACCTGCTGTATCAGTA
KanMX4 Internal Fwd	CGAGGCCGCGATTAAATTC
KanMX4Internal Rev	AAACTCACCGAGGCAGTTC
Primers for plasmid construction	
G-I Linker Upper	GCCAGAGGTATAGACATAGCCAGACCTACCTAATTGGTGCATCAGGTGGTCATGGCCCTTTATTCACGTAGACGGATAGG-TATAGCCAGACATCAGCAGCATACTTCGGGAACCGTAGGC
G-I Linker Lower	GCCTACGGTTCCCGAAGTATGCTGCTGATGTCTGGCTATACCTATCCGTCTACGTGAATAAAGGGCCATGACCACCTGATG-CACCAATTAGGTAGGTCTGGCTATGTCTATACCTCTGGC
Primers for verification of plasmid assembly	
Tag A amp Fwd	ATTATTGAAGCATTTATCAGGGTTATTGTCTCATG
Tag A amp Rev	GAAATGCTGGATGGGAAGCG
Tag B amp Fwd	GGCCCAATCACAACCACATC
Tag B amp Rev	GCATGTACGGGTTACAGCAGAATTAAAAG
Tag C amp Fwd	TGTACAAACGCGTGTACGCATG
Tag C amp Rev	CAGGTTGCTTTCTCAGGTATAGCATG
Tag D amp Fwd	ACTCTGTCATATACATCTGCCGCAC
Tag D amp Rev	GCTAAATGTACGGGCGACAG
Tag E amp Fwd	TTTCTCTTTCCCCATCCTTTACG
Tag E amp Rev	GTCGTCATAACGATGAGGTGTTGC
Tag F amp Fwd	GCCTTCATGCTCCTTGATTTCC
Tag F amp Rev	GGCGATCCCCCTAGAGTC
Tag G amp Fwd	AAAAGATACGAGGCGCGTGTAAG
Tag G amp Rev	CGCCTCGACATCATCTGCCCAG
Tag I amp Fwd	TGTTTTATATTTGTTGTAAAAAGTAGATAATTACTTCC
Tag I amp Rev	AGTCAGTGAGCGAGGAAGC

I-AmpR-A) to allow selection and propagation in both *S. cerevisiae* and *E. coli*. Plasmids propagated in *E. coli* were isolated with Sigma GenElute Plasmid Kit (Sigma Aldrich). Each cassette was flanked by unique restriction sites allowing them to be excised from the plasmid backbone. For digestion of each plasmid, high fidelity restriction endonucleases (Thermo Scientific) were used according to the manufacturer's instructions. pUD215 and pUD219 were digested with ApaI and EcoRV, pUD217 and pUD218 were digested with ApaI and BamHI, pUD216 was digested with SalI and SphI, pUD192 was digested with XhoI, pUD193 was digested with SacII, and pUD195 was digested with NotI. After digestion each fragment was purified by gel electrophoresis using 1% (w/v) agarose (Sigma Aldrich) in TAE buffer (40 mM Tris-acetate pH 8.0 and 1 mM EDTA). Isolation of agarose trapped DNA fragments was performed using Zymoclean Gel DNA Recovery Kit (Zymo Research). Equimolar amounts of each fragment were transformed into IMK504 (*dur1,2*Δ) allowing for in vivo vector assembly of pUDC121 and pUDE266 by homologous recombination. Correctly assembled

transformants were first selected on SMA agar, single colonies were then streaked onto SMU agar containing 20 nM $NiCl_2$. A single colony isolate with restored growth on urea was stocked and labelled as IMY082. Correct plasmid assembly was verified using primer pairs which bound in each of the gene cassettes and amplified the 60 bp homologous tags ("Primers for verification of plasmid assembly", Table 3). The plasmid was extracted from IMY082, named as pUDC121 and transformed into *E. coli* DH5α by electroporation in 2 mm cuvettes (1652086, BioRad, Hercules, CA) using a Gene PulserXcell electroporation system (BioRad) following the manufacturer's protocol and stocked in the *E. coli* host.

IMZ459 was constructed in the exact same manner as described for IMY082. However in place of a fragment containing the *nic1* gene cassette a 120 bp fragment with 60 bp homology to each adjacent cassette was used ("G-I linker upper and lower", Table 3). The resulting in vivo assembled plasmid was transformed into *E. coli* DH5α by electroporation and labelled as pUDE266.

2.3. Shake flask and chemostat cultivation

S. cerevisiae and *S. pombe* were grown in either SMA (Verduyn et al., 1990), SMU or SMS. When required, 20 nM $NiCl_2$ was added. If required, 150 mg/L uracil was added to the media. Cultures were grown in either 500 mL or 250 mL shake flasks containing 100 mL or 50 mL of synthetic medium and incubation at 30 °C in an Innova incubator shaker (New Brunswick Scientific, Edison, NJ) at 200 rpm. Optical density at 660 nm was measured at regular intervals using a Libra S11 spectrophotometer (Biochrom, Cambridge, United Kingdom). Controlled aerobic, carbon-limited chemostat cultivation was carried out at 30 °C in 2 L bioreactors (Applikon, Schiedam, The Netherlands) with a working volume of 1 L. Chemostat cultivation was preceded by a batch phase under the same conditions. When a rapid decrease in CO_2 production was observed (indicating glucose depletion), continuous cultivation at a dilution rate of 0.1 h^{-1} was initiated. Synthetic medium was supplemented with 7.5 g/L glucose and 0.2 g/L of Pluronic antifoam (BASF, Ludwigshaven, Germany). The pH was maintained constant at pH 5.0 by automatic addition of 2 M KOH and 2 M H_2SO_4. The stirrer speed was constant at 800 rpm and the aeration rate kept at 500 mL/min. Chemostat cultures were determined to be in steady state when after at least 5 volume changes the CO_2 production rate, O_2 consumption rate and cell dry weight had all varied by less than 2% over a period of 2 volume changes. Steady-state samples were taken between 12 and 15 volume changes after inoculation.

2.4. Analytical methods

96 well plate assays were prepared by adding 100 μL of SMA or SMU with 20 g/L glucose, 20 nM $NiCl_2$, Tween-80 (420 mg/L) and ergosterol (10 mg/L). If required, 10 mg/L histidine was added. Optical density was regularly measured at a wavelength of 660 nm in a GENios pro plate reader (Tecan Benelux, Giessen, The Netherlands). Cells were inoculated in each well to a starting $OD_{660\ nm}$ of 0.1. Plates were then covered with Nunc™ sealing tape (Thermo Scientific) and incubated at 30 °C with constant shaking at 200 rpm.

Biomass dry weight from bioreactors was determined by filtration of 10 mL broth over pre-dried and weighed 0.45 μm nitrocellulose filters (Gelman Laboratory, Ann Arbor, MI). After filtration the filters were dried for 20 min in a microwave at 350 W.

To determine extracellular glucose, urea and ammonium concentrations, samples were taken with the stainless steel bead method for rapid quenching of metabolism according to (Mashego et al., 2003). Culture samples were spun down at 3500*g* and the supernatant was collected. Extracellular metabolites were analysed using a Waters Alliance 2695 HPLC (Waters Chromatography B.V, Etten-Leur, The Netherlands) with an Aminex HPX-87H ion exchange column (BioRad) operated at 60 °C with a mobile phase of 5 mM H_2SO_4 and a flow rate of 0.6 mL/min. Extracellular urea concentrations were determined using GC–MS according to (de Jonge et al., 2011). Extracellular ammonium concentrations were determined using an Ammonium Cuvette test kit (Hach-Lange, Tiel, The Netherlands) according to the manufacturer's instructions.

The nitrogen content of the biomass was determined using Elemental Biomass Composition Analysis (EBCA). For this 150 mg of biomass were prepared by washing twice in MilliQ water (MilliQ) and resuspended in a total volume of 1 mL. After 48 h freeze drying, the biomass in the sample was crushed into a fine powder using a pestle and mortar. The pestle and mortar were prepared by autoclaving at 121 °C and thoroughly washed with subsequently 2 M H_2SO_4, 2 M KOH, MilliQ water (MilliQ) and acetone. Finally the pestle and mortar were dried at 100 °C for 24 h before use. The fine dried powder was then sent for analysis (ECN, Petten, The Netherlands) Total nitrogen was determined using a TOC-L CPH analyser (Shimadzu, 's-Hertogenbosch, The Netherlands) according to the manufacturer's instructions. In this method all nitrogen is first combusted to nitrogen monoxide, which is then detected by chemiluminescence using a non-dispersive infrared gas analyser.

2.5. Enzyme-activity assays

ATP-independent urease activity and urea amidolyase (ATP-dependent) activity was determined in two separate enzyme assays. Cell extracts were prepared by harvesting 62.5 mg of biomass dry weight by centrifugation at 4600*g* for 5 min. Cell pellets were washed with 10 mM potassium phosphate buffer containing 2 mM EDTA at pH 7.5, then washed again and resuspended in 100 mM potassium phosphate buffer at pH 7.5 containing 2 mM $MgCl_2$ and 2 mM dithiothreitol. Extracts were prepared using Fast Prep FP120 (Thermo Scientific) with 0.7 mm glass beads. Cells were desintegrated in 4 bursts of 20 s at speed 6 with 30 s of cooling on ice between each run. Cellular debris was removed by centrifugation at 47,000*g* for 20 min at 4 °C. The purified cell free extract was then used immediately for enzyme assays. Protein concentration of the cell extract was determined using the Lowry method (Lowry et al., 1951). Enzymatic assays were performed at 30 °C in a Hitachi U-3010 spectrophotometer. In both cases, activity of the urease enzyme was coupled to the conversion of ammonia to glutamate by glutamate dehydrogenase and the accompanying NADPH oxidation was monitored over time by a decrease in absorbance at 340 nm. ATP-independent urease activity was measured using a Urea/Ammonia rapid assay kit (Megazyme International Ireland, Wicklow, Ireland) with a modified protocol. The assay mixture contained in a total volume of 1 mL; 130 μL buffer solution, 80 μL NADPH solution, 20 μL glutamate dehydrogenase solution and cell extract. After allowing for residual enzymatic activity to subside, the reaction was initiated by addition of 50 mM urea. For determining ATP-dependent urease activity (urea amidolyase), the assay mixture contained in a total volume of 1 mL; 50 mM Tris–HCl pH8.0, 20 mM $KHCO_3$, 50 mM urea, 8 mM α-ketoglutarate, 15 mM KCl, 0.15 mM NADPH, 2.5 mM $MgCl_2$, 0.02 mM EDTA and 5 μL glutamate dehydrogenase solution from the urea/ammonia rapid assay kit (Megazyme). After allowing for residual activity to subside, the reaction was initiated by addition of 2 mM ATP.

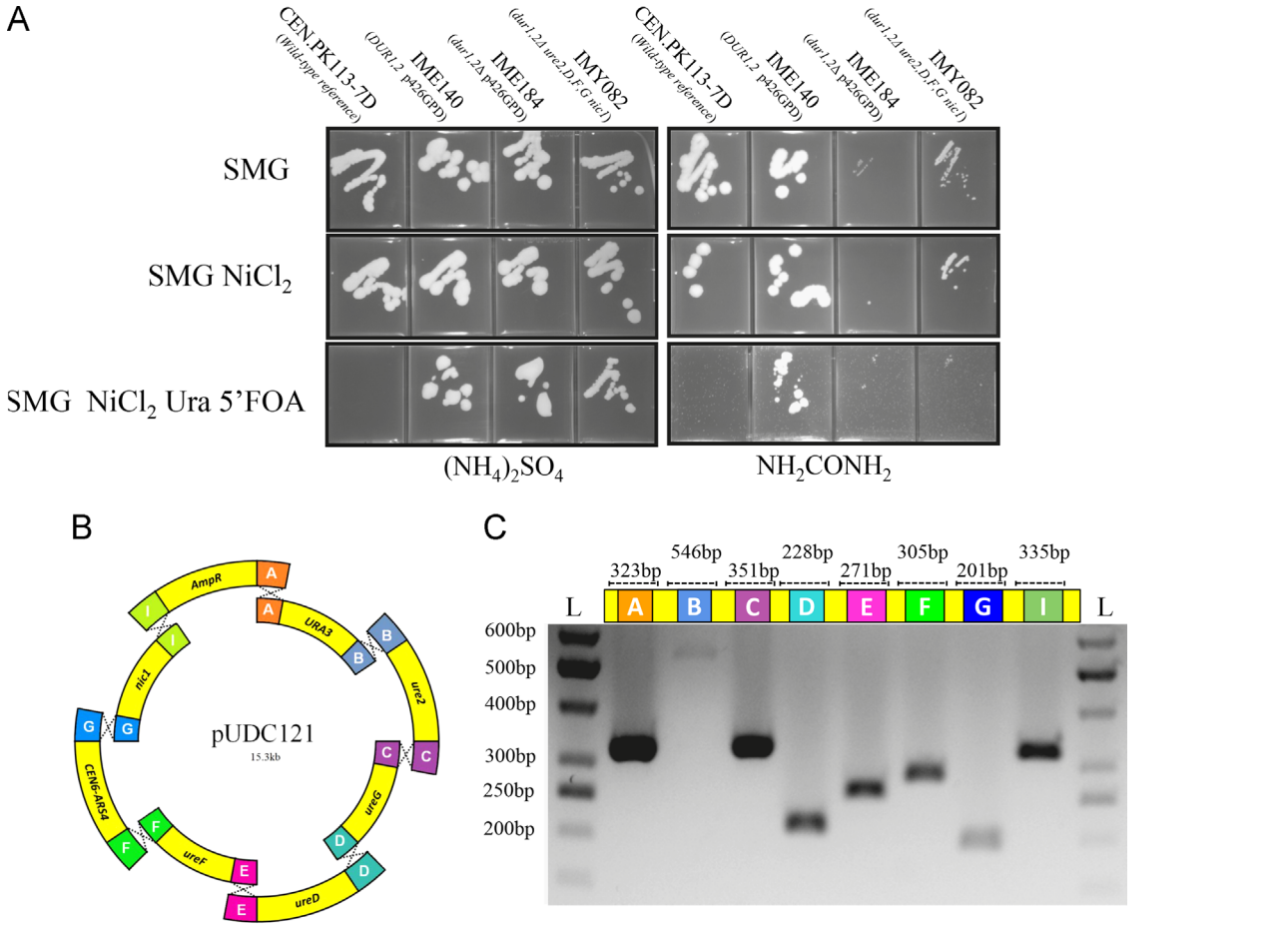

Fig. 2. (A) Complementation of *S. cerevisiae* IMK504 with pUDC121. Cells were plated on SMA or SMU agar with 20 nM $NiCl_2$, 0.150 g/L uracil (Ura) and 1 g/L 5-fluoroorotic acid (5′FOA) as indicated. Cells were pre-cultured in liquid synthetic medium with ammonium sulphate and washed twice in MilliQ water prior to plating. Plates were incubated aerobically for 72 h at 30 °C. (B) Outline of the assembly of pUDC121 using vector assembly by in vivo homologous recombination using 60 bp overlapping tags. (**C**) PCR analysis of the resulting plasmid pUDC121. PCR bands of the overlapping homologous tags were generated using primers which bound in each of the gene cassettes with the sizes indicated. L: DNA ladder.

2.6. Stoichiometric-model based prediction of the impact of urea assimilation on the biomass yield

The expected influence of the two different nitrogen sources and their uptake and utilization mechanisms were quantified by metabolic network analysis. In particular, the expected biomass yields were determined using a stoichiometric model containing 56 reactions (Supplementary information) and 52 balanced metabolites by optimization (linear programming) for a fixed substrate uptake rate ($v_{glc} = 1$):

$$\hat{v} = \underset{v}{\text{argmax}}(\, v_{biomass}) \text{ subject to} \left\{ \begin{array}{l} \mathbf{Sv} = \mathbf{0} \\ v_{glc} = 0 \\ \mathbf{v}_{irr} \geq 0 \end{array} \right\}$$

Where $\mathbf{v}$ is the vector of fluxes, $\mathbf{S}$ is the stoichiometric matrix of the model and $\mathbf{v}_{irr}$ is the set of irreversible fluxes. Urea was assumed to be transported passively on the basis that active transport is present only under urea-limiting conditions (Cooper and Sumrada, 1975). All calculations were performed using the tool CellNetAnalyzer (Klamt et al., 2007) using MATLAB linprog (MathWorks, Eindhoven, The Netherlands).

3. Results

3.1. Construction and selection of ATP-independent urea assimilation in S. cerevisiae

To engineer ATP-independent urea assimilation, the *S. cerevisiae DUR1,2* gene, which encodes an ATP-dependent urea amidolyase, was first deleted. The resulting strain IMK504 (*ura3-52, dur1,2*Δ) and the corresponding prototrophic strain IME184 (*ura3-52, dur1,2*Δ p426GPD) were unable to grow on urea as sole nitrogen source (Fig. 2A), thereby confirming that Dur1,2 is the only urea assimilation enzyme in *S. cerevisiae* (Cooper et al., 1980). Moreover, absence of growth on urea validated the strain as a suitable platform for a functional complementation study.

The coding sequences of the five *S. pombe* genes involved in functional expression of its ATP-independent urease were codon optimized for expression in *S. cerevisiae* using the JCat algorithm (Grote et al., 2005). These five genes comprised the urease structural gene *ure2*, as well as three urease accessory genes *ureD, ureF*, and *ureG*, and *nic1*, which encodes a high-affinity nickel transporter. While Ure2 is solely responsible for catalysing the conversion of urea to ammonia, *ureD, ureF*, and *ureG* are essential for its functional expression (Mobley et al., 1995). Although *S. cerevisiae* is not known to harbour nickel-dependent enzymes or a specific nickel transporter, it is well known that nickel ions can

enter *S. cerevisiae* cells when present at high concentrations (> 5 μM) (Joho et al., 1995). However, since addition of high concentrations of Ni^{2+} to growth media is undesirable and would likely result in nickel toxicity (Joho et al., 1995), *S. pombe nic1* (Eitinger et al., 2000) was co-expressed with the urease complex.

Construction of the ATP-independent urease strain IMY082 was achieved by in vivo vector assembly by homologous recombination (Kuijpers et al., 2013). In this approach, each heterologous gene cassette, comprising a strong constitutive promoter, a codon-optimized coding sequence and a terminator was flanked by 60 bp homologous tags which allowed adjacent cassettes with the same homologous tag to be assembled via in vivo homologous recombination (Kuijpers et al., 2013). With the addition of a cassette for the *URA3* marker, the *CEN6ARS4* yeast replicon and an *E. coli* fragment including the ampicillin resistance gene (ampR) and a bacterial origin of replication, the yeast expression plasmid pUDC121 was assembled in vivo in the strain IMK504 (*ura3-52*, *dur1,2*Δ) resulting in strain IMY082 (*dur1,2*Δ, *ure2,D,F,G nic1*). Correct assembly of the corresponding plasmid (pUDC121) (Fig. 2B) was confirmed by PCR (Fig. 2C).

To assess the ability of the ATP-independent urease construct to support growth of the resulting strain IMY082 (*dur1,2*Δ, *ure2,D,F,G nic1*) on urea, it was initially plated on synthetic medium with ammonium and, subsequently, replica plated onto synthetic medium containing urea as the sole nitrogen source and supplemented with 20 nM $NiCl_2$ (Fig. 2A). IMY082 grew on media supplemented with urea and $NiCl_2$, while the negative control strain IME184 (*dur1,2*Δ, p426GPD) grew on synthetic medium with ammonium, but not with urea as the nitrogen source. The reference strains CEN.PK113-7D (*DUR1,2*) and IME140 (*DUR1,2 ura3-52* p426GPD (*URA3*)) grew normally on both ammonium and urea media. Strain IMY082 did not grow on SMU agar plates that were supplemented with 5′fluoroorotic acid (5FOA) to induce plasmid loss. This observation further confirmed that, indeed, the heterologous plasmid was responsible for growth on urea and functionally complemented the *dur1,2* deletion (Fig. 2A).

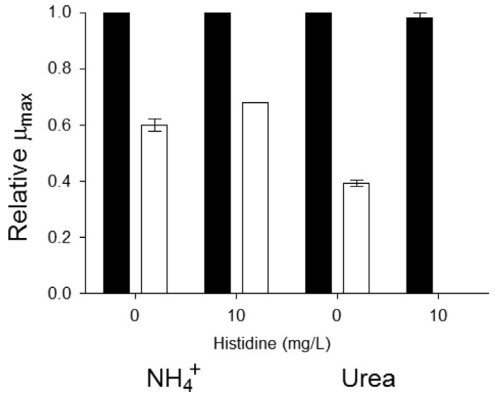

Fig. 3. Relative maximum specific growth rates of IME140 (*DUR1,2* p426GPD) (black bars) and IMY082 (*dur1,2*Δ *ure2,D,F,G nic1*) (white bars) in SMA (NH_4) or SMU (Urea) with 20 nM $NiCl_2$, Tween-80 (420 mg/L), ergosterol (10 mg/L) with 0 mg/L and 10 mg/L histidine. Cells were cultured in 100 μl volumes in a 96 well plate and incubated at 30 °C with OD660 measured at 15 min intervals. Data are presented as averages and standard deviations of triplicate experiments, relative to the average maximum specific growth rate of IME140 under each condition.

3.2. Nickel dependency of *S. cerevisiae* IMY082 (*dur1,2*Δ, *ure2,D,F,G nic1*)

The engineered *S. cerevisiae* strain IMY082 (*dur1,2*Δ, *ure2,D,F,G nic1*) grew on urea without addition of Ni^{2+} to the growth medium (Fig. 2A) and continued to grow on urea after 10 successive serial transfers in media that had not been supplemented with Ni^{2+}. The introduced urea assimilation system requires only one nickel atom per urease enzyme to become catalytically active (Mobley et al., 1995) suggesting that only trace amounts of Ni^{2+} are required for urease activity. This raised the possibility that nickel contamination from glassware and medium components might have been sufficient to support growth of the engineered strain. To test this hypothesis, a series of growth assays were performed in the presence of histidine. Histidine is a strong chelator of nickel (histidine/Ni^{2+} dissociation constant $K_D = 14 \pm 1$ nM) (Knecht et al., 2009) and is involved in nickel detoxification in *S. cerevisiae* (Joho et al., 1995). Growth rates of the ATP-independent urease strain (IMY082) and the ATP-dependent urease reference strain (IME140) were compared by monitoring OD_{660nm} in 96-well plates in synthetic media (SMA and SMU) supplemented with anaerobic growth factors Tween-80/ergosterol and 20 nM $NiCl_2$ in the presence (10 mg/L) and absence of histidine. Both strains showed comparable growth rates with ammonium sulphate as the sole nitrogen source at both histidine concentrations tested (Fig. 3). During growth on urea the control strain IME140 showed comparable growth rates at both histidine concentrations tested. However, for IMY082, growth on urea was only observed in the cultures to which no histidine had been added and 10 mg/L histidine completely abolished growth (Fig. 3). This result confirmed that, also after expression in *S. cerevisiae*, the ATP-independent urease from *S. pombe* has a strict requirement for nickel. Additionally, this indicates that even without supplementation of $NiCl_2$, the synthetic medium used in this study already contains sufficient nickel to support growth of the engineered strain on urea.

Table 4
Aerobic maximum specific growth rates in shake-flask cultivations containing 100 mL SMA and SMU with $NiCl_2$ supplementation as indicated. Shown are averages and mean deviations from two replicates. NG: No growth, ND: Not determined.

Media	Strains				
	IME140 (*DUR1,2* p426GPD)	IMY082 (*dur1,2*Δ *ure2,D,F,G nic1*)	IMZ459 (*dur1,2*Δ *ure2,D,F,G*)	IME184 (*dur1,2*Δ p426GPD)	*S. pombe* 7264 (*ure2,D,F,G nic1*[a])
NH_4^+	0.33 ± 0.01	0.16 ± 0.01	0.14 ± 0.01	ND	ND
NH_4^+ + 20 nM $NiCl_2$	0.30 ± 0.02	0.19 ± 0.01	0.14 ± 0.01	ND	ND
NH_4^+ + 20 μM $NiCl_2$	0.30 ± 0.02	0.18 ± 0.01	0.16 ± 0.01	ND	ND
Urea	0.31 ± 0.02	0.18 ± 0.00	NG	NG	ND
Urea + 20 nM $NiCl_2$	0.32 ± 0.00	0.18 ± 0.00	NG	NG	0.15 ± 0.00
Urea + 20 μM $NiCl_2$	0.28 ± 0.01	0.20 ± 0.00	0.16 ± 0.00	NG	ND

[a] Genes expressed under their own native promoter.

Table 5
Specific enzyme activities for ATP-dependent and ATP-independent ureases in *S. cerevisiae* and *S. pombe* cell extracts grown on SMA and SMS supplemented with 20 nM $NiCl_2$. Specific activity is expressed in μmol min^{-1} mg $protein^{-1}$. Data are presented as averages and mean deviations from two biological replicates. NA: not applicable (strain does not grow on urea), BD: below detection limit of 0.01 μmol min^{-1} mg $protein^{-1}$).

Strain	ATP-dependent		ATP-independent	
	Urea	Serine	Urea	Serine
IME184 (*dur1,2*Δ p426GPD)	NA	BD	NA	BD
IME140 (*DUR1,2* p426GPD)	0.05 ± 0.01	BD	BD	BD
S. pombe 7264 (*ure2,D,F,G nic1*[a])	BD	BD	0.06 ± 0.00	BD
IMY082 (*dur1,2*Δ *ure2,D,F,G nic1*)	BD	BD	0.44 ± 0.01	0.32 ± 0.02

[a] Genes expressed from their native promoter.

Table 6
Predicted biomass yields of the ATP-dependent urease control strain IME140 (*DUR1,2* p426GPD) and ATP-independent urease strain IMY082 (*dur1,2*Δ *ure2,D,F,G nic1*) under aerobic and anaerobic glucose limited chemostat conditions with both NH_4^+ and urea as the sole nitrogen source. Values were calculated based on a stoichiometric model optimized for maximal biomass production. All yield values are expressed as g biomass/g glucose.

Condition	N-source	Strain		Improvement (%)
		IME140	IMY082	
Aerobic	NH_4^+	0.5364	0.5364	0
	Urea	0.5360	0.5471	2.1
Anaerobic	NH_4^+	0.1035	0.1035	0
	Urea	0.1060	0.1088	2.6

3.3. Functionality of the Nic1 transporter

In *S. pombe*, Nic1 transports nickel across the plasma membrane and into the cytosol with high affinity. However in the absence of the Nic1 transporter, nickel is still able to cross the membrane via non-specific metal uptake systems, particularly via magnesium transporters (Eitinger et al., 2000). A similar situation is observed in *S. cerevisiae* where nickel can enter the cell through non-specific metal uptake systems, particularly via the magnesium transporters Alr1 and Alr2 (MacDiarmid and Gardner, 1998). In *S. cerevisiae*, wild-type cells have been reported to accumulate 19.9 nmol Ni^{2+}/mg biomass in the presence of 0.1 mM $NiCl_2$ (Nishimura et al., 1998).

To study the functionality of *nic1* in the engineered strain, especially at low concentrations of Ni^{2+} in growth media, an ATP-independent urease strain was constructed which lacked the *nic1* expression cassette. Analogous to the construction of strain IMY082, this strain was built using vector assembly by homologous recombination (Kuijpers et al., 2013). The expression cassettes of the *S. pombe* urease complex (but lacking the *nic1* cassette) were assembled in vivo in the *dur1,2*Δ strain IMK504, yielding in plasmid pUDE266. In place of the *nic1* cassette, a 120 bp fragment with 60 bp homology to each adjacent cassette was used, yielding the strain IMZ459 (*dur1,2*Δ, *ure2,D,F,G*). After confirmation of correct assembly by PCR, growth of strain IMZ459 was analysed on synthetic medium with urea as the sole nitrogen source and with different concentrations of $NiCl_2$. In media with added $NiCl_2$ concentrations ranging from 0 nM to 1 μM, no growth was observed. However, at a concentration of 20 μM $NiCl_2$, the strain grew on urea medium with a specific growth rate of 0.16 ± 0.00 h^{-1} (Table 4).

To quantitatively determine the effect and potential benefit of the Nic1 transporter, specific growth rates of IMY082 (with *nic1*) and IMZ459 (no Ni-transporter), as well as an ATP-dependent urease control (IME140) were determined from cultures growing in SMU and SMA in the presence of 0 nM, 20 nM, and 20 μM of added $NiCl_2$ (Table 4). While both IME140 and IMY082 were able to grow under all conditions tested, IMZ459 (no Ni-transporter) could only grow on urea in the presence of 20 μM $NiCl_2$. The ability of the strain containing the Nic1 transporter to grow at > 1000 fold lower concentrations of NiCl2 compared to the negative control strain IMZ459 confirmed the functional expression of the Nic1 transporter.

3.4. ATP-independent urease enzyme activity

After confirmation of the activity and Ni^{2+}-dependency of *S. pombe ure2* expressed in *S. cerevisiae*, the ATP-(in)dependency and enzyme activities of both the native and heterologous urease enzyme were investigated in cell extracts of different strains. In these experiments, strains were pre-grown in synthetic medium containing either urea or serine as the sole nitrogen source to determine the impact of nitrogen source on urease activity. Serine was chosen as an alternative nitrogen source instead of ammonium sulphate so that trace amounts of ammonium remaining in the cell free extract would not interfere with the enzyme assays. Irrespective of the nitrogen source used for growth, ATP-independent urease activity was measured in cell-free extracts of the engineered strain IMY082 (*dur1,2*Δ, *ure2,D,F,G nic1*). ATP-independent urease activities in cell extracts of urea- and serine-grown of this strain were comparable (0.44 ± 0.01 and 0.32 ± 0.02 μmol min^{-1} mg $protein^{-1}$, respectively) (Table 5). Activity of the heterologously expressed *S. pombe* urease in *S. cerevisiae* was ca. six-fold higher than the enzyme activity observed in urea-grown cultures of *S. pombe* (0.06 ± 0.00 μmol min^{-1} mg $protein^{-1}$). Consistent with the deletion of the native *S. cerevisiae* urease gene *DUR1,2,* no ATP-dependent urease activity was detected in cell extracts of strain IMY082, irrespective of the nitrogen source. Cell extracts of the ATP-dependent urease control strain (IME140, *DUR1,2*) only exhibited activity in the presence of ATP, with a specific activity of 0.05 ± 0.01 μmol min^{-1} mg $protein^{-1}$ (Table 5).

3.5. Physiological characterisation

To study the quantitative impact of the replacement of the native *S. cerevisiae* ATP-dependent urease with a heterologous ATP-independent urease, the physiology of strains IMY082 (*dur1,2*Δ, *ure2,D,F,G nic1*) and IME140 (*DUR1,2*) were compared in glucose-grown shake-flask and chemostat cultures with urea or ammonium as the sole nitrogen sources.

Irrespective of the nitrogen source, the engineered strain IMY082 grew 30–50% slower than the control strain in shake flask cultures (Table 4). Increasing the concentration of $NiCl_2$ (up to 20 μM) had no significant impact on the specific growth rate on urea or ammonium as nitrogen sources.

Chemostat cultivation allows for physiological comparison of strains with different maximum specific growth rates at identical sub-maximal specific growth rates (dilution rates) determined by the operator (Tai et al., 2005). Aerobic glucose-limited chemostat cultures of strains IMY082 (*dur1,2*Δ, *ure2,D,F,G nic1*) and IME140 (*DUR1,2*) were run at a dilution rate of 0.10 h^{-1} in synthetic medium with either ammonium or urea as the nitrogen source, in all cases supplemented with 20 nM $NiCl_2$. ATP conservation during urea assimilation should theoretically result in an increase in biomass yield as the conserved ATP can be used for biomass production. While cultivation under anaerobic conditions would theoretically result in the largest relative increase in biomass yield (2.6% as compared to 2.1% under aerobic conditions) (Table 6), both values are within the error limit of the biomass determinations in chemostat cultures. In ammonium-grown, glucose-limited

Table 7
Physiology of the ATP-dependent urease strain IME140 (*DUR1,2* p426GPD) and the ATP-independent urease strain IMY082 (*dur1,2Δ ure2,D,F,G nic1*) in aerobic glucose limited chemostat cultures in SMA and SMU with 7.5 g/L glucose and 20 nM $NiCl_2$ maintained at pH 5.0 and a dilution rate of 0.1 h^{-1}.

Parameters	Urea+Ni		NH_4^++Ni	
	IME140[a]	IMY082[a]	IME140[b]	IMY082[b]
Dilution rate (h^{-1})	0.10 ± 0.00	0.10 ± 0.00	0.10 ± 0.00	0.10 ± 0.01
Yx/s (g/g glucose)	0.50 ± 0.01	0.50 ± 0.01	0.49 ± 0.00	0.49 ± 0.00
qO_2 (mmol/g/ h)	2.76 ± 0.07	2.78 ± 0.13	2.77 ± 0.15	2.59 ± 0.05
qCO_2 (mmol/g /h)	3.24 ± 0.02	3.30 ± 0.10	2.75 ± 0.25	2.64 ± 0.12
qGlucose (mmol/g/ h)	1.07 ± 0.03	1.10 ± 0.03	1.12 ± 0.03	1.05 ± 0.03
qUrea/NH_4^+ (mmol/g/h)	0.41 ± 0.01	0.46 ± 0.01[c]	0.35 ± 0.05	0.36 ± 0.09
Residual NH_4^+ (mM)	10.38 ± 0.20	17.20 ± 0.21	NA	NA
Nitrogen in biomass (mg/g biomass)	67.5 ± 0.5	56.0 ± 1.0	72.0[d]	ND
C recovery (%)	104 ± 1.7	103 ± 0.8	100 ± 3.0	103 ± 1.5
N recovery (%)[e]	96 ± 0.8	97 ± 0.3	105 ± 5.6	106 ± 3.7

NA: not applicable; ND: not determined.

[a] Averages and mean deviations from two replicates.
[b] Averages and standard deviations from three replicates.
[c] Calculated from residual urea values from one chemostat.
[d] Based on CEN.PK113-7D data from (Lange and Heijnen, 2001).
[e] Calculated from nitrogen balance presented in Supplementary data 2.

chemostat cultures, no statistically significant differences were observed in relevant physiological parameters between IMY082 (*dur1,2Δ*, *ure2,D,F,G nic1*) and IME140 (*DUR1,2*) (Table 7). Also on urea, biomass-specific fluxes and biomass yields of IMY082 and IME140 were not significantly different. However, whilst both strains released some ammonium after intracellular conversion of urea, this ammonia release was ca. 70% higher in strain IMY082 than in IME140 (17.20 ± 0.21 mM vs 10.38 ± 0.2 mM). Additionally, a lower nitrogen content of the biomass was measured for the engineered strain (56.0 ± 1.0 mg/g biomass) than for IME140 (67.5 ± 0.5 mg/g biomass). Given the differences in nitrogen distribution observed for IME140 and IMY082 at steady state, an accurate account of nitrogen distribution was made. The nitrogen balances of the chemostat cultivations (Supplementary data 2) nearly closed to 100% when extracellular urea, ammonium, and nitrogen in the biomass were compared with the urea fed to the cultures. A closed nitrogen balance was also observed when total nitrogen analyses on the reservoir medium at the time of steady-state sampling, the supernatant at steady state, and the whole cell broth at steady state were compared.

4. Discussion

4.1. Expression of a Ni-dependent ATP-independent urease in S. cerevisiae

In this study, we demonstrate the functional replacement of the native *S. cerevisiae* ATP-dependent urea assimilation enzyme (Dur1,2) by an ATP-independent enzyme from *S. pombe* (Ure2) and three accessory proteins (UreF, UreG and UreD; Bacanamwo et al., 2002), which were previously shown to be essential for functional enzymatic activity in organisms expressing ATP-independent urease (Lee et al., 1992; Park et al., 2005).

Although the catalytic mechanisms of urea hydrolysis in *S. cerevisiae* and *S. pombe* differ significantly, both systems lead to ammonia and carbon dioxide formation (Fig. 1).

In fungi there is an evolutionary divergence between organisms that assimilate urea at the expense of ATP and those that do not. Yeasts belonging to the subphylum *Saccharomycotina* (e.g. *S. cerevisiae*) (Kurtzman and Robnett, 2013; Weiss et al., 2013) harbour the *DUR1,2* gene encoding ATP-dependent urease. It has been hypothesized that the evolutionary advantage of expending ATP was to allow yeasts such as *S. cerevisiae* to eliminate all nickel-requiring reactions, thus reducing the number of transition metals for which cellular homoeostasis and regulation is required (Navarathna et al., 2010). In this study, we demonstrate that co-expression of the *S. pombe* high affinity Ni^{2+}-transporter gene (Nic1; Eitinger et al., 2000) was required for Ure2-dependent growth of *S. cerevisiae* at low Ni^{2+} concentrations. This is in line with phylogenetic research, which indicates that acquisition of the bi-functional ATP-dependent Dur1,2 and loss of ATP-independent urease in the ancestor of *Saccharomycotina* yeasts coincided with the loss of the high affinity nickel transporter (Navarathna et al., 2010; Zhang et al., 2009).

Although the growth of a *dur1,2Δ S. cerevisiae* strain on urea could be restored by complementation of the *S. pombe* urease system, the engineered strain (IMY082) exhibited a growth rate decrease ranging from ca. 30% to 50% depending on the growth conditions relative to a *DUR1,2* reference strain (Table 4). Surprisingly, this decreased growth rate was not only observed during growth on urea, but also on ammonium, a condition in which urease is not expected to be involved in nitrogen assimilation. Overexpression of the native *DUR1,2* gene, leading to enzyme activities comparable to those measured with the *S. pombe* enzyme in our study, did not result in a reduction of the growth rate (Coulon et al., 2006) suggesting that increased urease activity is not the cause for the suboptimal growth. Moreover, release of ammonia by the cultures indicates that the capacity of the heterologous enzyme was sufficient to sustain the ammonia requirement for growth.

In the current metabolic engineering design, heterologous genes were placed under the control of highly active glycolytic promoters (Knijnenburg et al., 2009). While placing *ure2*, the catalytic enzyme behind such a promoter may be useful to enable high in vivo fluxes, the high expression of the accessory enzymes might not be necessary and, in contrast, may have led to an increased general protein burden (Sauer et al., 2014) and/or interference with metal metabolism and homoeostasis or protein folding. Future strain designs should take this possibility into account by either fine tuning individual gene expression by selecting appropriate promoters (Blazeck et al., 2012; Nevoigt et al., 2006) or by evolutionary and reverse engineering to select strains with recovered growth rates (Oud et al., 2012).

4.2. Functional expression of nickel dependent enzymes in S. cerevisiae

The present study demonstrates that functional expression of a heterologous Ni-dependent activity in the *S. cerevisiae* cytosol is possible and not precluded by, for example, binding of Ni by cytosolic histidine. This result represents an innovation in the metabolic engineering of this yeast with possible implications beyond engineering of urea metabolism. Ni-containing enzymes play critical roles in bacteria, archaea, fungi, algae, and higher plants (Mulrooney and Hausinger, 2003), but encompass a limited range of activities (i.e. glyoxalase I, acidreductone dioxygenase, urease, superoxide dismutase, [NiFe]-hydrogenase, carbon monoxide dehydrogenase, acetyl-coenzyme A synthase/decarbonylase, methyl-coenzyme M reductase and lactase racemase) (Boer et al., 2014). In addition, as reported in this study for the *S. pombe* urease, the Ni-dependent enzymes require auxiliary proteins that participate in Ni delivery, metallocenter assembly, or organometallic cofactor synthesis and a dedicated transport system (Higgins et al., 2012). Having demonstrated the successful expression of a functionally active Ni-dependent urease, other Ni-dependent enzymes might also be functionally expressed in *S. cerevisiae*. As an example, the optimization of the formation of cytosolic acetyl-CoA as a precursor for many industrially produced chemicals (isoprenoids, lipids, butanol, flavonoids) in *S. cerevisiae* has recently received a lot of attention (Krivoruchko et al., 2015). This includes the successful replacement of yeast acetyl-CoA synthases by several ATP-independent solutions encompassing the cytosolic expression of the ATP-independent pyruvate dehydrogenase complex (PDH) from *Enterococcus faecalis* (Kozak et al., 2014b), and the expression of an acetylating acetaldehyde dehydrogenase and the expression of a pyruvate-formate lyase (Kozak et al., 2014a). In all these cases acetyl-CoA is formed from intermediates of central metabolism, acetate or pyruvate. In contrast, acetogenic microorganisms such as *Moorella thermoacetica* use the Ni^{2+}-dependent acetyl-CoA decarboxylase/synthase (Mulrooney and Hausinger, 2003) to catalyse the reversible formation of acetyl-CoA from CO_2, Co-enzymeA and a corrinoid-bound methyl group (Maynard and Lindahl, 1999), resulting in net CO_2 fixation. While implementation of this pathway into *S. cerevisiae* will involve major other challenges – e.g. engineering of vitamin B12 biosynthesis into this eukaryote – the demonstration that Ni-dependent enzymes can be expressed in this yeast eliminates at least one potential hurdle.

4.3. Decreasing the ATP requirement for nitrogen-containing products

The elimination of the ATP requirement for urea assimilation decreases the ATP requirement by 0.5 mol of ATP per mol of nitrogen assimilated. In this study, urea was solely used as a nitrogen source for the formation of biomass. Based on stoichiometric model-based predictions, the decreased requirement for ATP in urea assimilation under aerobic conditions could result in an increase of the biomass yield on glucose of 2.1%. Although potentially relevant for large scale yeast biomass production, this small predicted increase is within the error margin of the biomass yield determinations on glucose in our laboratory chemostat cultures (Table 7). Additionally, excretion of ammonia into the extracellular space, which has previously been reported for urea-grown wild-type cultures of *S. cerevisiae* (Marini et al., 1997), may decrease the positive impact of ATP-independent urease. If the exported ammonia re-associates with a proton to form ammonium and is then take up again, this might cause a futile cycle due to the energy costs of ammonium uptake (Fig. 1). These results indicate that, in order to fully benefit from the ATP savings during urea assimilation in strains expressing ATP-independent urease, its expression should be tuned to prevent ammonia release into the medium.

The potential benefit of ATP-independent nitrogen assimilation can be much larger in strains that not only require nitrogen for biomass formation, but also for the formation of nitrogen containing products. The yeast *S. cerevisiae* has widely been used as a host for the production of heterologous proteins (e.g. human insulin) (Cousens et al., 1987; Kazemi et al., 2013a; Kazemi et al., 2013b; Walsh, 2005). Considering that the production of 1 mol of heterologous human insulin requires approximately 66 mol of NH_3 (based on the total amino acid sequence), the conservation of a corresponding 33 mol of ATP (amount of ATP required to produce 66 mol of NH_3 from urea using ATP-dependent Dur1,2) would result in a reduction of 2.06 mol of glucose consumed per mol of human insulin produced (assuming aerobic conditions and a P/O-ratio of 1.0; Bakker et al., 2001). An even more drastic impact on product formation is expected for anaerobic production of nitrogen-containing low-molecular-weight compounds such as amino acids. For example, homofermentative production, by an engineered *S. cerevisiae* strain, of alanine from glucose and ammonium is expected to have a net ATP yield of zero, since the ATP costs for ammonium uptake would exactly cancel out ATP synthesis in glycolysis. Since ATP is needed for growth and maintenance, this would preclude an anaerobic production process. Conversely, ATP independent-urea assimilation would result in a net ATP yield of 1 mol per mol alanine, which is equivalent to the ATP yield from alcoholic fermentation and should therefore enable a robust anaerobic process. Altering the energetics of nitrogen assimilation represents a first step in engineering *S. cerevisiae* as a metabolic engineering platform for energy-efficient production of nitrogen containing commodity chemicals such as diamines or amino acids.

Acknowledgments

This work was performed within the BE-Basic R&D Program (http://www.be-basic.org/), which was granted an FES subsidy from the Dutch Ministry of Economic Affairs, Agriculture and Innovation (EL&I). The authors wish to thank Erik de Hulster, Jeroen Koendjbiharie, Angela ten Pierick and Patricia van Dam for their assistance on this project.

Appendix A. Supplementary material

Supplementary data associated with this article can be found in the online version at http://dx.doi.org/10.1016/j.ymben.2015.05.003.

References

Albright, E.D., 2000. Encyclopedia of food microbiology, 3 vols. Library J. 125 (90-90).
Bacanamwo, M., Witte, C.P., Lubbers, M.W., Polacco, J.C., 2002. Activation of the urease of *Schizosaccharomyces pombe* by the UreF accessory protein from soybean. Mol. Genet. Genomics 268, 525–534.
Bakker, B.M., Overkamp, K.M., Maris, A.J., Kötter, P., Luttik, M.A., Dijken, J.P., Pronk, J.T., 2001. Stoichiometry and compartmentation of NADH metabolism in *Saccharomyces cerevisiae*. FEMS Microbiol. Rev. 25, 15–37.
Blazeck, J., Garg, R., Reed, B., Alper, H.S., 2012. Controlling promoter strength and regulation in *Saccharomyces cerevisiae* using synthetic hybrid promoters. Biotechnol. Bioeng. 109, 2884–2895.
Boer, J.L., Mulrooney, S.B., Hausinger, R.P., 2014. Nickel-dependent metalloenzymes. Arch. Biochem. Biophys. 544, 142–152.
Carter, E.L., Tronrud, D.E., Taber, S.R., Karplus, P.A., Hausinger, R.P., 2011. Iron-containing urease in a pathogenic bacterium. Proc. Natl. Acad. Sci. USA 108, 13095–13099.
Cooper, T.G., Lam, C., Turoscy, V., 1980. Structural analysis of the *dur* loci in *S. cerevisiae*: two domains of a single multifunctional gene. Genetics 94, 555–580.
Cooper, T.G., Sumrada, R., 1975. Urea transport in *Saccharomyces cerevisiae*. J. Bacteriol. 121, 571–576.

Coulon, J., Husnik, J., Inglis, D., van der Merwe, G., Lonvaud, A., Erasmus, D., vanVuuren, H., 2006. Metabolic engineering of *Saccharomyces cerevisiae* to minimize the production of ethyl carbamate in wine. Am. J. Enol. Vitic. **57**, 113–124.

Cousens, L.S., Shuster, J.R., Gallegos, C., Ku, L.L., Stempien, M.M., Urdea, M.S., Sanchez-Pescador, R., Taylor, A., Tekamp-Olson, P., 1987. High level expression of proinsulin in the yeast, *Saccharomyces cerevisiae*. Gene 61, 265–275.

de Jonge, L.P., Buijs, N.A.A., ten Pierick, A., Deshmukh, A., Zhao, Z., JAKW, Kiel, Heijnen, J.J., Gulik, W.M., 2011. Scale-down of penicillin production in *Penicillium chrysogenum*. Biotechnol. J. **6**, 944–958.

de Kok, S., Kozak, B.U., Pronk, J.T., van Maris, A.J., 2012. Energy coupling in *Saccharomyces cerevisiae*: selected opportunities for metabolic engineering. FEMS Yeast Res. 12, 387–397.

Eitinger, T., Degen, O., Bohnke, U., Muller, M., 2000. Nic1p, a relative of bacterial transition metal permeases in *Schizosaccharomyces pombe*, provides nickel ion for urease biosynthesis. J. Biol. Chem. 275, 18029–18033.

Entian, K.D., Kötter, P., 2007. Yeast genetic strain and plasmid collections. Method Microbiol. 36, 629–666.

Gietz, R.D., Woods, R.A., 2002. Transformation of yeast by lithium acetate/single-stranded carrier DNA/polyethylene glycol method. Method Enzymol. 350, 87–96.

Grote, A., Hiller, K., Scheer, M., Munch, R., Nortemann, B., Hempel, D.C., Jahn, D., 2005. JCat: a novel tool to adapt codon usage of a target gene to its potential expression host. Nucleic Acids Res. 33, W526–W531.

Guldener, U., Heck, S., Fielder, T., Beinhauer, J., Hegemann, J.H., 1996. A new efficient gene disruption cassette for repeated use in budding yeast. Nucleic Acids Res. 24, 2519–2524.

Hensing, M.C.M., Bangma, K.A., Raamsdonk, L.M., Dehulster, E., Vandijken, J.P., Pronk, J.T., 1995. Effects of cultivation conditions on the production of heterologous alpha-galactosidase by *Kluyveromyces lactis*. Appl. Microbiol. Biotechnol. 43, 58–64.

Hermann, T., 2003. Industrial production of amino acids by coryneform bacteria. J. Biotechnol. 104, 155–172.

Higgins, K.A., Carr, C.E., Maroney, M.J., 2012. Specific metal recognition in nickel trafficking. Biochemistry 51, 7816–7832.

Hong, K.K., Nielsen, J., 2012. Metabolic engineering of *Saccharomyces cerevisiae*: a key cell factory platform for future biorefineries. Cell Mol. Life Sci. 69, 2671–2690.

Ikeda, M., 2003. Amino acid production processes. Adv. Biochem. Eng. Biotechnol. 79, 1–35.

Joho, M., Inouhe, M., Tohoyama, H., Murayama, T., 1995. Nickel resistance mechanisms in yeasts and other fungi. J. Ind. Microbiol. 14, 164–168.

Kazemi, S.A., Cruz, A.L., de, H.E., Hebly, M., Palmqvist, E.A., van, G.W., Daran, J.M., Pronk, J., Olsson, L., 2013a. Long-term adaptation of *Saccharomyces cerevisiae* to the burden of recombinant insulin production. Biotechnol. Bioeng. 110, 2749–2763.

Kazemi, S.A., Palmqvist, E.A., Schluckebier, G., Pettersson, I., Olsson, L., 2013b. The challenge of improved secretory production of active pharmaceutical ingredients in *Saccharomyces cerevisiae*: a case study on human insulin analogs. Biotechnol. Bioeng. 110, 2764–2774.

Klamt, S., Saez-Rodriguez, J., Gilles, E.D., 2007. Structural and functional analysis of cellular networks with CellNetAnalyzer. BMC Syst. Biol. 1 (2), 2–8.

Knecht, S., Ricklin, D., Eberle, A.N., Ernst, B., 2009. Oligohis-tags: mechanisms of binding to Ni^{2+}–NTA surfaces. J. Mol. Recognit. 22, 270–279.

Knijnenburg, T.A., Daran, J.M., van den Broek, M.A., Daran-Lapujade, P.A., de Winde, J.H., Pronk, J.T., Reinders, M.J., Wessels, L.F., 2009. Combinatorial effects of environmental parameters on transcriptional regulation in *Saccharomyces cerevisiae*: a quantitative analysis of a compendium of chemostat-based transcriptome data. BMC Genomics 10, http://dx.doi.org/10.1186/1471-2164-10-53.

Kozak, B.U., van Rossum, H.M., Benjamin, K.R., Wu, L., Daran, J.M., Pronk, J.T., van Maris, A.J., 2014a. Replacement of the *Saccharomyces cerevisiae* acetyl-CoA synthetases by alternative pathways for cytosolic acetyl-CoA synthesis. Metab. Eng. 21, 46–59.

Kozak, B.U., van Rossum, H.M., Luttik, M.A., Akeroyd, M., Benjamin, K.R., Wu, L., de VS, Daran JM, Pronk, J.T., van Maris, A.J., 2014b. Engineering acetyl coenzyme A supply: functional expression of a bacterial pyruvate dehydrogenase complex in the cytosol of *Saccharomyces cerevisiae*. mBio **5**, 8–14.

Krivoruchko, A., Zhang, Y., Siewers, V., Chen, Y., Nielsen, J., 2015. Microbial acetyl-CoA metabolism and metabolic engineering. Metab. Eng. 28, 28–42.

Kuijpers, N.G., Solis-Escalante, D., Bosman, L., van den Broek, M., Pronk, J.T., Daran, J.M., Daran-Lapujade, P., 2013. A versatile, efficient strategy for assembly of multi-fragment expression vectors in *Saccharomyces cerevisiae* using 60 bp synthetic recombination sequences. Microb. Cell Fact. 12 (47-12).

Kurtzman, C.P., Robnett, C.J., 2013. Relationships among genera of the *Saccharomycotina* (*Ascomycota*) from multigene phylogenetic analysis of type species. FEMS Yeast Res. 13, 23–33.

Lange, H.C., Heijnen, J.J., 2001. Statistical reconciliation of the elemental and molecular biomass composition of *Saccharomyces cerevisiae*. Biotechnol. Bioeng. 75, 334–344.

Lee, M.H., Mulrooney, S.B., Renner, M.J., Markowicz, Y., Hausinger, R.P., 1992. *Klebsiella aerogenes* urease gene cluster: sequence of *ureD* and demonstration that four accessory genes (*ureD, ureE, ureF*, and *ureG*) are involved in nickel metallocenter biosynthesis. J. Bacteriol. 174, 4324–4330.

Lowry, O.H., Rosebrough, N.J., Farr, A.L., Randall, R.J., 1951. Protein measurement with the folin phenol reagent. J. Biol. Chem. 193, 265–275.

Lucet, D., Le Gall, T., Mioskowski, C., 1998. The chemistry of vicinal diamines. Angew. Chem. Int. Edit. 37, 2581–2627.

MacDiarmid, C.W., Gardner, R.C., 1998. Overexpression of the *Saccharomyces cerevisiae* magnesium transport system confers resistance to aluminum ion. J. Biol. Chem. 273, 1727–1732.

Marini, A.M., Soussi-Boudekou, S., Vissers, S., Andre, B., 1997. A family of ammonium transporters in *Saccharomyces cerevisiae*. Mol. Cell. Biol. 17, 4282–4293.

Mashego, M.R., van Gulik, W.M., Vinke, J.L., Heijnen, J.J., 2003. Critical evaluation of sampling techniques for residual glucose determination in carbon-limited chemostat culture of *Saccharomyces cerevisiae*. Biotechnol. Bioeng. 20, 395–399.

Maynard, E., Lindahl, J., 1999. Evidence of a molecular tunnel connecting the active sites for CO2 reduction and acetyl-CoA synthesis in acetyl-CoA synthase from *Clostridium thermoaceticum*. J. Am. Chem. Soc. 121, 9221–9222.

Mobley, H.L., Island, M.D., Hausinger, R.P., 1995. Molecular biology of microbial ureases. Microbiol. Rev. 59, 451–480.

Mulrooney, S.B., Hausinger, R.P., 2003. Nickel uptake and utilization by microorganisms. FEMS Microbiol. Rev. 27, 239–261.

Mumberg, D., Muller, R., Funk, M., 1995. Yeast vectors for the controlled expression of heterologous proteins in different genetic backgrounds. Gene 156, 119–122.

Navarathna, D.H., Harris, S.D., Roberts, D.D., Nickerson, K.W., 2010. Evolutionary aspects of urea utilization by fungi. FEMS Yeast Res. **10**, 209–213.

Nevoigt, E., Kohnke, J., Fischer, C.R., Alper, H., Stahl, U., Stephanopoulos, G., 2006. Engineering of promoter replacement cassettes for fine-tuning of gene expression in *Saccharomyces cerevisiae*. Appl. Environ. Microbiol. 72, 5266–5273.

Nijkamp, J.F., van den Broek, M.A., Datema, E., et al., 2012. *De novo* sequencing, assembly and analysis of the genome of the laboratory strain *Saccharomyces cerevisiae* CEN.PK113-7D, a model for modern industrial biotechnology. Microb. Cell Fact. 11, 36–42.

Nishimura, K., Igarashi, K., Kakinuma, Y., 1998. Proton gradient-driven nickel uptake by vacuolar membrane vesicles of *Saccharomyces cerevisiae*. J. Bacteriol. 180, 1962–1964.

Ostergaard, S., Olsson, L., Nielsen, J., 2000. Metabolic engineering of *Saccharomyces cerevisiae*. Microbiol. Mol. Biol. Rev. 64, 34–50.

Oud, B., van Maris, A.J., Daran, J.M., Pronk, J.T., 2012. Genome-wide analytical approaches for reverse metabolic engineering of industrially relevant phenotypes in yeast. FEMS Yeast Res. 12, 183–196.

Park, J.U., Song, J.Y., Kwon, Y.C., et al., 2005. Effect of the urease accessory genes on activation of the *Helicobacter pylori* urease apoprotein. Mol. Cells **20**, 371–377.

Pronk, J.T., 2002. Auxotrophic yeast strains in fundamental and applied research. Appl. Environ. Microbiol. 68, 2095–2100.

Qian, Z.G., Xia, X.X., Lee, S.Y., 2009. Metabolic engineering of *Escherichia coli* for the production of putrescine: a four carbon diamine. Biotechnol. Bioeng. 104, 651–662.

Qian, Z.G., Xia, X.X., Lee, S.Y., 2011. Metabolic engineering of *Escherichia coli* for the production of cadaverine: a five carbon diamine. Biotechnol. Bioeng. 108, 93–103.

Sauer, M., Branduardi, P., Rußmayer, H., Marx, H., Porro, D., Mattanovich, D., 2014. Production of Metabolites and Heterologous Proteins. In: Piskur, J., Compagno, C. (Eds.), Springer-Verlag, Berlin Heidelberg, pp. 299–321.

Tai, S.L., Boer, V.M., Daran-Lapujade, P., Walsh, M.C., de Winde, J.H., Daran, J.M., Pronk, J.T., 2005. Two-dimensional transcriptome analysis in chemostat cultures - Combinatorial effects of oxygen availability and macronutrient limitation in *Saccharomyces cerevisiae*. J. Biol. Chem. 280, 437–447.

Verduyn, C., Postma, E., Scheffers, W.A., van Dijken, J.P., 1992. Effect of benzoic acid on metabolic fluxes in yeasts: a continuous-culture study on the regulation of respiration and alcoholic fermentation. Yeast 8, 501–517.

Verduyn, C., Postma, E., Scheffers, W.A., Vandijken, J.P., 1990. Physiology of *Saccharomyces cerevisiae* in anaerobic glucose-limited chemostat cultures. J. Gen. Microbiol. 136, 395–403.

Walsh, G., 2005. Therapeutic insulins and their large-scale manufacture. Appl. Microbiol. Biotechnol. 67, 151–159.

Weiss, S., Samson, F., Navarro, D., Casaregola, S., 2013. YeastIP: a database for identification and phylogeny of *Saccharomycotina* yeasts. FEMS Yeast Res. 13, 117–125.

Weusthuis, R.A., Lamot, I., van der Oost, J., Sanders, J.P.M., 2011. Microbial production of bulk chemicals: development of anaerobic processes. Trends Biotechnol. 29, 153–158.

Wu, G., 2009. Amino acids: metabolism, functions, and nutrition. Amino Acids 37, 1–17.

Xun Yao Chen, 2014. An investor's guide to nitrogen fertilizers: key 2014 drivers, ⟨http://marketrealist.com/2014/03/investors-guide-to-nitrogen-fertilizers-key-drivers-1q2014/⟩.

Zhang, Y., Rodionov, D.A., Gelfand, M.S., Gladyshev, V.N., 2009. Comparative genomic analyses of nickel, cobalt and vitamin B12 utilization. BMC Genomics 10, 78.